Schweizerische Mineralogische und Petrographische Mitteilungen 84, 3–24, 2004

Understanding and assessing European mineral resources – a new approach using GIS Central Europe

Daniel Cassard[1], *Andor L.W. Lips*[1], *Jean-Marc Leistel*[1], *Yann Itard*[1], *Nicole Debeglia-Marchand*[2], *Laurent Guillou-Frottier*[1], *Wim Spakman*[3], *Gilbert Stein*[1] and *Yves Husson*[1]

Abstract

The GIS (Geographic Information System) Central Europe, in support of the Alpine-Balkan-Carpathian-Dinarides (ABCD) GEODE Project, is composed of spatially referenced geographical, geological, geophysical, geochemical and mineral deposit thematic layers, and their respective attribute data. It has been created to establish insights in the region's mineral potential and its past and future mining activities, and to determine parameter combinations that control the spatial-temporal distribution of the ore deposits. To contribute to the sustainability of the mining industry, environmental data are also integrated in the information system, allowing a regional scale risk assessment for old and new mining projects.

The data analysis and synthesis, required to arrive at the different thematic layers, already highlight parameters that may be tentatively linked to ore deposit formation and localization. The assessment and compilation of heat flow data show a large anomalous area of high heat flow, located within the Pannonian basin, adjacent to the east Carpathians with anomalously low heat flow values. Such high contrasts in the thermal regime in the crust may play a role in the ore genesis. The compilation of multisource gravity information has returned enhanced gravity maps, Bouguer and isostatic anomalies, gravity gradients and gravity discontinuities. Linked in with the earthquake epicenter distribution, these layers contribute to a better understanding of the crustal structure, regionally with the topo-isostatic anomaly map and more locally with the vertical gradient anomaly map. The present-day structure of the crust, completed by the structure of the lithosphere, e.g. with the 3-D seismic tomography visualization, allows to verify the region's geodynamic evolution. The 3-D visualization (and the correlation with the heat flow thematic layer) reconfirms the preferred positioning of Neogene (Au) deposits above shallow low velocity bodies. The visualization also suggests that (subducted) lithosphere underlying these low velocity bodies obstructs the emplacement of the deposits (e.g. Aegean arc and mainland Greece), unless this subducted lithosphere has been positioned at/around the 660 km discontinuity (Rhodope and Apuseni regions). Geodynamically this observation can be explained by the insufficient influx of asthenospheric heat in the narrow mantle wedges above shallow subducted lithosphere. In relation to the geodynamic setting certain ore deposit types mark the tectono-magmatic evolution of the Tethys and the Carpatho-Balkan arc. Oceanic type mineralizations (chromite, Cu massive sulphides) formed during the oceanic rifting from Jurassic to Upper Cretaceous, and hydrothermal-porphyry types (base- and precious-metal mineralizations) formed during two major stages, during the Cretaceous to Paleogene, and subsequently during the Neogene.

Linked in with information on materials processing (waste production and management, toxicity information), land use, infrastructure in/around mining districts, and other socio-economic information help the GIS to evolve towards a modern tool for the sustainable management of mineral resources in southeastern Europe.

Keywords: GIS, metallogeny, environment, prediction map, Central and South-Eastern Europe.

1. The architecture of GIS Central Europe

GIS Central Europe, drawing heavily on the authors' experience in creating GIS Andes (Cassard, 1999; Cassard et al., 2001a), comprises three modules (Cassard et al., 2001b); (i) Geography, (ii) Geology & Mining, and (iii) Environment (Table 1). The thematic layers in the first two modules center around four group themes; geography, geology, geophysics, and resources. The third module includes a descriptive section, which is currently made up of four layers: land-use and

[1] Mineral Resources Division, BRGM, 3 avenue Claude Guillemin - BP 6009 - 45060 Orléans cedex 2, France. E-mail to <d.cassard@brgm.fr>.
[2] Development Planning and Natural Risks Division, BRGM, Orléans, France.
[3] Vening Meinesz Research School of Geodynamics, Utrecht University, the Netherlands.

0036-7699/04/0084/3

Fig. 1 Heat flow values present in the Heat Flow layer of the GIS Central Europe, after selection and classification among the available data (IHFC database and recently published values). Arbitrary contouring delineates areas of anomalously high and low heat flow values (dark gray and light gray contours respectively).

land cover, meteorology and environmental monitoring, human settlements, and industrial areas. The descriptive section is linked to a non-geographic database on potential polluting substances, activity sectors using potentially polluting products, and relevant national and international regulations and standards. This database also contains extensive data, complementary to the existing ore deposit information layer theme, to estimate the potential environmental impact of different ore deposits; e.g. on the geochemical signatures of the main deposit types, the heavy-metal content of all minerals, and chemical descriptions of rock types.

1.1. Projection system

The GIS is presented in a Transverse Mercator projection system (datum WGS84, Central Meridian 21°E, reference latitude 0, scale factor 1, FE 1000000, FN 0). The present configuration was preferred with respect to e.g. a Lambert Conform Conic map projection because of the relatively large total distance from north to south (from south Poland to Crete), which would create further geometric distortions in projections of the outer areas of the GIS.

1.2. Geology

In the development of the GIS for Central Europe a homogeneous geological coverage for the whole ABCD-GEODE[1] region has been established. The coverage has been created by synthesizing published national geological maps (scales 1:200,000 to 1:500,000) and regional thematic maps (scales 1:500,000 to 1:1,500,000) after applying a standardized legend based on the age and the lithology of the mapped units, with 54 stratigraphic boxes and 35 lithologic overprint patterns. The scales of the used input maps certify the precision of the synthesis at a 1:1,500,000 scale and allow an optimal regional integration with other coverages in the GIS (mineral deposits, geothermal resources, geophysics, etc.). The coverage further benefits from the geochronology database allowing to link published radiometric data to the respective host polygons. As such the homogeneous synthesis will serve as an ideal basis for geologic, tectonic and geodynamic investigations covering the whole ABCD region.

[1] The GEODE acronym refers to the ESF funded programme "Geodynamics and Ore Deposit Evolution". ABCD-GEODE indicates the subprogramme concerned with the Alpine-Balkan-Carpathian-Dinarides region.

1.3. Geochronology

The geochronology presented in the GIS Central Europe is derived from data published between 1980 and 2000 and currently contains some 850 data points. As for most other databases this application under Microsoft Access® benefits from in-house developed lexicons, in this case concerning lithology, minerals, and lithostratigraphic units. In addition, small lexicons were created hierarchizing the analytical method and the geological significance. The existing lexicons minimize typo-errors and allow the application of various queries to the data. Parallel to the bibliography listing pointing to the source of the original data, the data include a unique ID of every data point, its location, quality (presenting an expert's view qualification of the registration: good, acceptable, reasonable, doubtful; determined by the published information about the analytical quality, the geological significance and the sample description and location), local rock name, dated object, lithology, deposit name (if cross-correlated with the mineral deposit database), dated mineral(s), applied isotope technique, age, analytical aspects (internal error, intercept, MWSD, amount per sample), and original sample code (following the coding of the author of the published information).

1.4. Geophysics

1.4.1. Heat flow

An up-to-date synthesis of available heat flow data in Central Europe has been performed. The global compilation of terrestrial heat flow data, carried out in 1991 by the International Heat Flow Commission (IHFC database, Pollack et al., 1993), and recent published data (Cermak et al., 1996; Pfister et al., 1998) have been integrated to provide a large-scale map of the equilibrium thermal regime in Central Europe (Fig. 1). After the compilation stage, a critical analysis of the 963 available data points has been made, according to the internationally recognized criteria for ranking quality of heat flow measurements. In brief, where several deep boreholes are used returning consistent heat flow determinations along several hundreds of meters, a "high quality" is assigned. When standard deviation between two neighboring boreholes exceeds 30%, a "low quality" is assigned. The "medium quality" corresponds to reasonable standard deviations, but where estimates have been made in shallow depth intervals, or when thermal conductivity values are not necessarily well constrained, or when a single borehole

Table 1 Thematic layers of the GIS Central Europe "Geography" and "Geology & Mining" modules.

Module	Group	Layer theme	Description
Geography	Geography	**Geography**	A Digital Chart of the World (DCW)® geographic base, including political boundaries, towns, villages, hydrography, infrastructures, etc.
		DEM	Two digital elevation models: one oceanic (2-minute arc), and one continental (30-second arc) elevation data set with structural analysis of the detailed topography calculated maps
		Imagery	SPOT 4 VEGETATION® satellite images at 1x1 km
Geology & Mining	Geology	**Geological map coverage**	Present state of geological coverage: location of and information on the existing maps
		Geological synthesis	Synthetic geological map of Central and Southeastern Europe at 1:1,500,000 scale
		Simplified geological map	Simplified geological map of Central and Southeastern Europe at 1:1,500,000 scale with characterization of morpho-structural domains and main tectonic elements
		Volcanism	Data on Holocene volcanism
		Geochemistry	Composition and age of magmatic and volcanic rocks — isotope data
		Geochronology	Synthesis of existing data, methods used, critical analysis, reliability, references, etc.
	Geophysics	**Heat flow**	An up-to-date synthesis
		Gravimetry	Bouguer anomaly calculation; isostatic correction and corresponding residual anomalies; vertical gradient calculation and structural analysis
		Seismics	Distribution of earthquakes in order to better understand and constrain the crustal structures
		Moho	Depth contour map
		3D Tomography	3D model of the lithospheric structure (cooperation with Utrecht University)
	Resources	**Geothermal resources**	Based on inventories at present being compiled for the EU
		Ore deposits	Providing information on 1) location, company, local names, links to other databases, 2) geology, host rock (+ age), deposit type (+ age), using a new metallogenic lexicon, and including mineralogical (ore, gangue and hydrothermal alteration), fluid-inclusion and isotopic data of the main ore deposits, 3) economy, exploitation type, production reserves, resources per commodity, 4) bibliography
		Mining districts	Delimitation, magmatic and structural controls, potential and information on mining companies
Environment	Land & climate	**Land-use & land cover**	Detailed administrative boundaries showing environmentally protected areas such as national parks ; land-use (agriculture, forest, urbanism, industry, mine waste, etc.), mainly determined from satellite imagery
		Meteorology & Environmental monitoring	Climate, quality monitoring networks for water, groundwater, air and soils, and also vulnerability to risks and natural hazards (e.g. flooding, earthquakes, etc.)
	Population & industry	**Human settlements**	Distribution and characterization of human activities (highlighting socioeconomic aspects)
		Industrial areas	Pollution sources (with inventories and characterization) in the different activity sectors

is used. 18% of the 673 continental data (thus excluding heat flow data from the Black and Mediterranean Seas), have been assigned a low quality, and only 11% (74 data) can be considered as high quality data.

Since one objective of the integrated GIS study is to highlight large-scale geodynamic processes, it was necessary to average heat flow data measured in a small area. Values that were separated by only a few kilometers in the IHFC database were clustered in the GIS Central Europe thematic layer in order to keep an averaged value for one site, representative of the local thermal regime (up to 10 km × 10 km). Consequently, the short wavelength heat flow variations are smoothed out, leaving only long wavelength heat flow variations, attributable to changes in the deep thermal regime. The description of long wavelength signatures probably involves deep thermal processes, which have to be considered with other long wavelength signatures, such as gravity anomalies or crustal thickness variations (see next section). It must be pointed out that a similar map with only high quality data would confirm these long wavelength signatures (not shown here, but included in Fig. 1 when only considering the data points indicated by circles).

Figure 1 shows continental and oceanic heat flow values collected for the GIS Central Europe, together with their quality. The information allows to (arbitrarily) discriminate areas where terrestrial heat flow is higher or lower than "normal" (dark gray and light gray contours respectively). The largest anomalously high heat flow area is delimited by the Pannonian Basin and some smaller areas can be identified around Greek basins (e.g. the Strymon Basin). Areas of low heat flow data can be identified in eastern Italy, in Albania and towards the Russian platform. Remarkable is the opposite thermal signature inferred on each side of the eastern Carpathians. The thermal signature resembles the deeper thermal reflection of the heat flow compilation by Nemcock et al. (1998) and Tari et al. (1999), showing a similar overall picture. These studies have not been included in our compilation because of

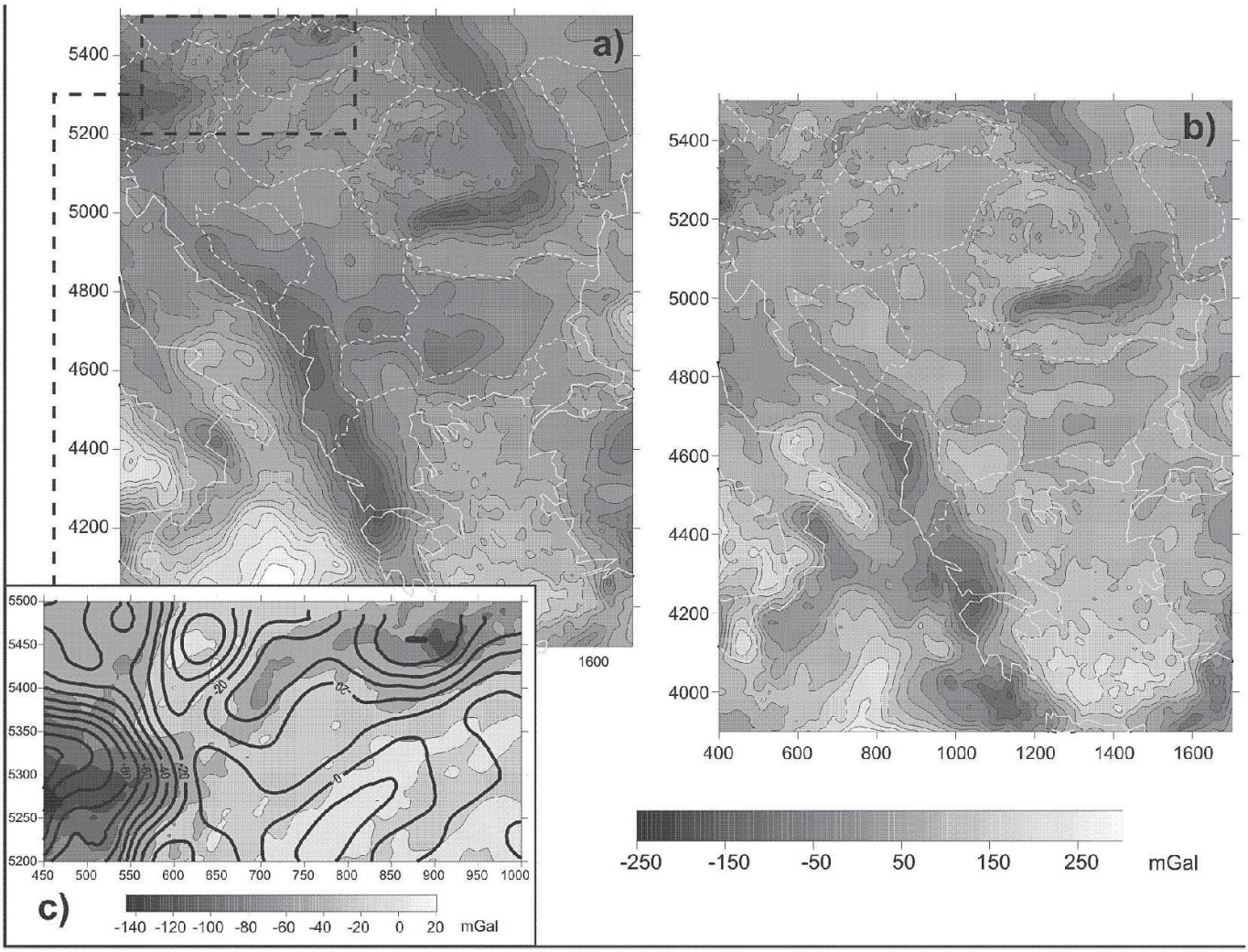

Fig. 2 Ground gravity data information supplemented with satellite data. (a) Composite Bouguer anomaly map. (b) Topo-isostatic anomaly map. (c) Comparison of the ground (underlying image) and satellite (overlying contours) Bouguer anomalies in a test zone.

the absence of vital information to assess plotted heat flow values as reliable heat flow data. The contrasting large anomalous area of high heat flow, located within the Pannonian basin, with a region of anomalously low heat flow values (east Carpathians) and the relative high heat flow may have played an important role in the ore genesis.

1.4.2. Gravity

The compilation of multisource gravity information has returned enhanced gravity maps, Bouguer and isostatic anomalies, gravity gradients and gravity discontinuities. The gravity data was mainly obtained from the Bureau Gravimétrique International (BGI) in the form of gravimetric stations (Table 2) or as grids (Table 3). For the station data, the accuracy of the Simple Bouguer provided by the BGI varies between countries (the estimated error is always less than 5 mGal). For Poland, digitized data was added from the Gravimetric Atlas of Poland (Krolikowski and Petecki, 1995). All these data were first converted in the simple Bouguer and IGSN 71 system, with a standard 1967 gravity formula.

Where no ground-measured gravity data are available (e.g. ex-Yugoslavia, Greece, Turkey and offshore), satellite data from the Scripps Institution of Oceanography were incorporated. These data include:

– Off-shore, the marine gravity data are the 2-minute anomaly grid developed by D.T. Sandwell, using Geosat and ERS 1 satellite altimetric data. A comparison with the marine gravity data obtained using vessels indicates that the accuracy of the satellite anomalies is on average 4 to 7 mGal (Sandwell and Smith, 1997); this increases to 3 mGal when the trajectory of the vessel follows the trajectory established for a Geosat/ERM (Exact Repeat Mission).

– On-shore, the data are derived from the geopotential model EGM96 (NASA 1998), based on trajectometry data. With wavelengths greater than 100 km, it can only provide information (i) at a regional scale and (ii) related to deep-lying structures (Fig. 2c).

A Digital Terrain Model on a 5-minute mesh (ETOPO5 grid), obtained from the National Geophysical Data Centre (NGDC) was used for grid conversions and calculation of topographic corrections.

The Bouguer anomaly map (Fig. 2a) is characterized by strong negative anomalies along the Carpathian arc, Eastern Alps, Dinarides and west-

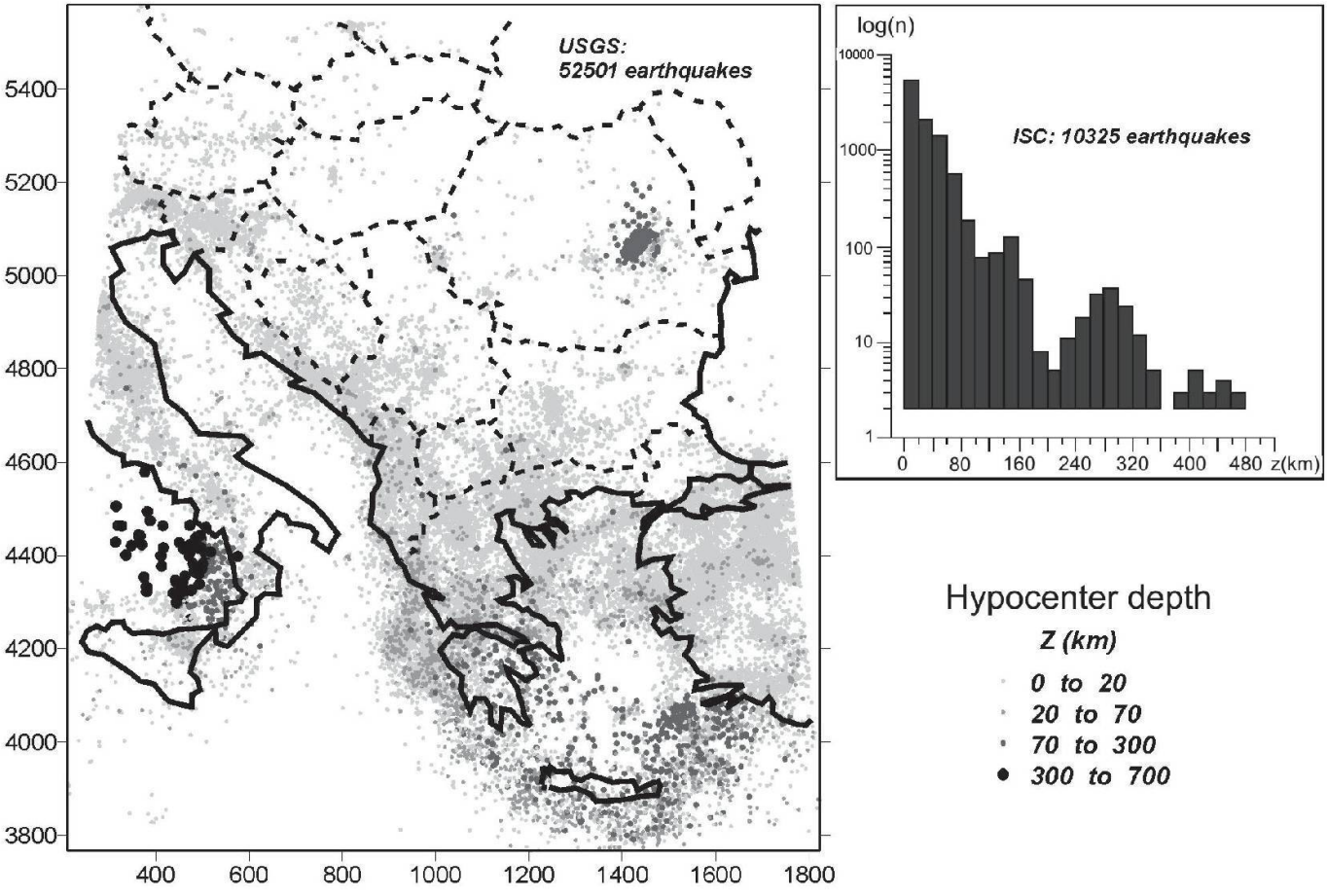

Fig. 3 Hypocenter depth distribution map and histogram (sources USGS - http://wwwneic.cr.usgs.gov/neis/epic/database.html; ISC - http://www.isc.ac.uk/Bull).

Table 2 Gravimetric stations available from the BGI.

Country	Number of stations	Mean density of stations (per km^2)
Austria	11301	0.13
Hungary	636	0.007
Czech Rep. & Slovakia	972	0.008
Poland	1315	Very low in the south
Romania	123	Very low
Greece	219	Very low
Turkey	228	Very low

Table 3 Gravimetric grids available from the BGI.

Country	Mesh	Anomaly	Reference system	Standard gravity	Number of initial stations
Hungary	7.5'*5'	Free-air	Potsdam	Cassinis 1930	unknown
Czech Rep. & Slovakia	7.5'*5'	Free-air and Bouguer	IGSN71 ?	GRS80	unknown
Poland	5'*5'	Free-air	Potsdam	GRS80	Unknown
Romania	7.5'*5'	Bouguer (2.67) TC: radius 20 and 400 km Accuracy: 0.1 mGal	IGSN71 ?	Cassinis 1930 Krasovsky ellipsoid	78026 (mean density 0.33 km^{-2})
USSR	1°*1°	Free-air	IGSN71	1967 formula	unknown

ern Rhodope Mountains. In contrast, the Pannonian and Danube basins are marked by positive regional anomalies of 20 mGal on average. Very strong positive anomalies of up to 300 mGal appear in the Mediterranean basin.

The distribution of the gravity anomalies shows a strong correlation with topography and bathymetry due to significant isostatic effects. Deep seismic survey data of the Carpathian arc (Zatopek, 1979; Krus and Sutora, 1986; Nemcok et al., 1998; Tari et al., 1999) have resolved a crustal root whose depth varies between 40 km towards Krakow to 50 km in the southern Carpathians. The crust would, however, be thinned to 25 km beneath the Pannonian basin. A root of 50 km is also apparently present beneath the eastern end of the Alpine arc. Due to the absence of a homogeneous coverage of seismic data for the entire area under study crustal depths were derived for a local compensation model, based on the Airy and Heiskanen hypotheses and the corresponding isostatic corrections were computed.

On land, the residual isostatic anomalies (Fig. 2b) are still negative over some of the Carpathian arc, particularly in its southern part, whereas they are positive in the basins. The anomalies indicate the divergence to local isostatic equilibrium, evidenced by the descent of the Vrancea lithospheric slab into the asthenosphere and by induced basin subsidence and volcanism (Chalot-Prat and Girbacea, 2000). Locally, residual anomalies could be related to shallow density heterogeneities such as thick molasse formations along the arc, thickness variations of sediments in the basins or mixed volcanism ranging from low-density acidic to mafic rocks.

Linked in with the earthquake epicenter distribution (next section), the gravity theme layers contribute to a better understanding of the crustal structure, regionally with the topo-isostatic anomaly map and more locally with the vertical gradient anomaly map.

1.4.3. Seismics

The distribution, focal depths and magnitude of earthquakes, complemented by focal mechanism data, were extracted from international earthquake databases in order to better understand the crustal structures (Fig. 3).

– A total of 52,501 valid earthquakes were extracted from the USGS Earthquake database. The focal depths of the retained earthquakes varied from 0 to 501 km, with a mean of 14 km. The deep-

est earthquakes are located in the Tyrrhenian Sea. Other deep earthquakes position in the Vrancea area of Romania, and along the Aegean arc.

–A total of 10,325 earthquakes, recorded from 1964 to 1999 and sorted from other agencies' databases in order to select the most reliable information, were extracted from the International Seismological Center database. The focal-depth histogram shows a three modal distribution, with most of the foci being at less than 20 km depth, an intermediate group centered on 300 km depth and some deep foci at more than 380 km.

– A total of 6,993 recent earthquakes recorded from 1998 to 2000 were extracted from the Euro Mediterranean Seismological Center database. The EMSC database also gives access to data on the focal mechanisms (Double Couple Solution) calculated at the GeoForschungsZentrum (GFZ) in Potsdam.

– Focal mechanism data were also extracted from the Harvard Seismology CMT database and from the ETH Zürich SMT database, giving insight into the present day crustal dynamics.

In conclusion, the distribution of epicenters shows the overall shallow position of most earthquakes. With exception of the southeastern Carpathians (Vrancea region) and the Aegean arc, all epicenters tend to fall in the crustal portion of the lithosphere. The detailed analysis of these shallow earthquakes (in combination with the gravity theme layers) help to position crustal structures that may have contributed to the ore formation by localizing fluid circulation. The present-day structure of the crust, completed by the structure of the lithosphere, e.g. with the 3-D seismic tomography visualization (next section), allows to verify the region's crustal reflection to the overall geodynamic evolution.

1.4.4. Tomography

The tomography presented in the GIS Central Europe is derived from a global travel-time tomographic dataset developed at the Vening Meinesz Research School of Geodynamics in Utrecht, the Netherlands (Bijwaard et al., 1998). Basic theory and related equations are presented by Spakman (1993). The tomography is derived from a global irregular parameterization (based on hit count patterns) and a non-linear inversion of P-wave (first) arrivals, incorporating 3-D ray tracing, station statistics, and accurate hypocenter determination, simultaneously (Bijwaard et al., 1998; Bijwaard and Spakman, 2000).

The data in the GIS represents a regularly gridded subset of datapoints from the global model at 0.6 degrees horizontal intervals (28 rows by 28 columns; northwest corner at 50.10N13.3E) and at 12 different depth levels, at 17.5, 52.5, 95.0, 145.0, 200.0, 260.0, 320.0, 380.0, 440.0, 500.0, 562.5, and 627.5 kilometers, respectively. The three dimensional organization of datapoints, which represent the relative travel time residuals (varying between –4.2% and +4.3% at the 17.5 kilometer level to –1.3% and +1.9% at the 627.5 kilometer level), has been interpolated in three dimensions by applying in-house developed modeling software to obtain 3-D isocontours of the tomographic values (Courrioux et al., 2001). The 3-D model allows importation of other thematic layers from the GIS and can be easily navigated with a VMRL web viewer.

The 3-D visualization does not introduce new phenomena which have not been reported before in published studies (e.g. consult Wortel and Spakman, 2000, for a review). However, the visualization supports further insights in the extension,

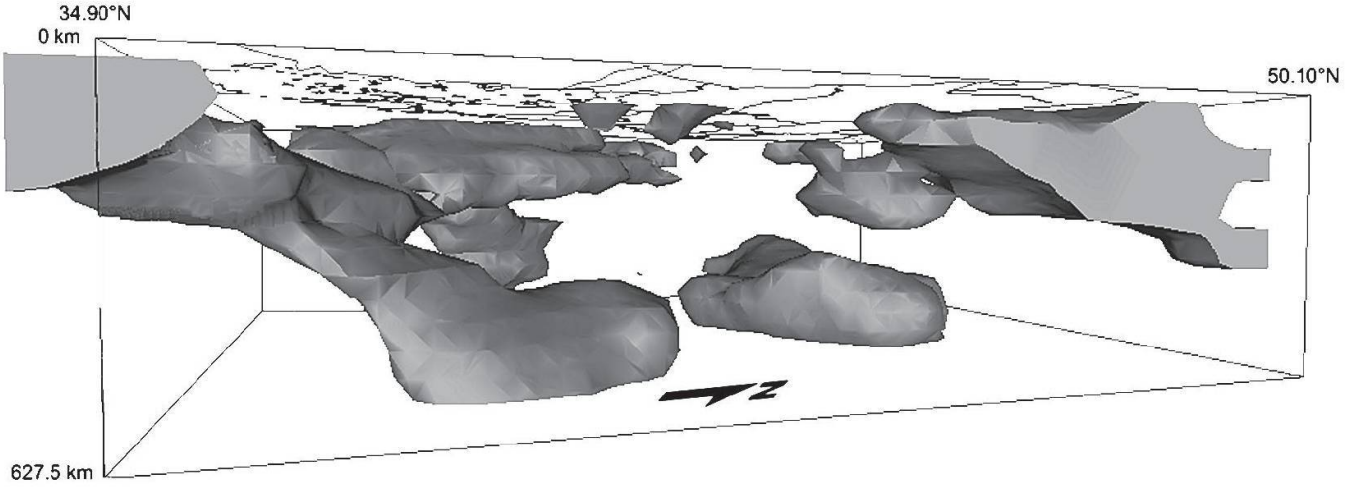

Fig. 4 3D visualization of seismic tomography below southeastern Europe viewed from the east. 3D bodies indicate values above 1% anomalies. Image shows east European platform (upper right), continuous Hellenic subduction zone with flat portion at 600–650 km, and a similar flat lying body below the Pannonian region (disconnected from the east European platform).

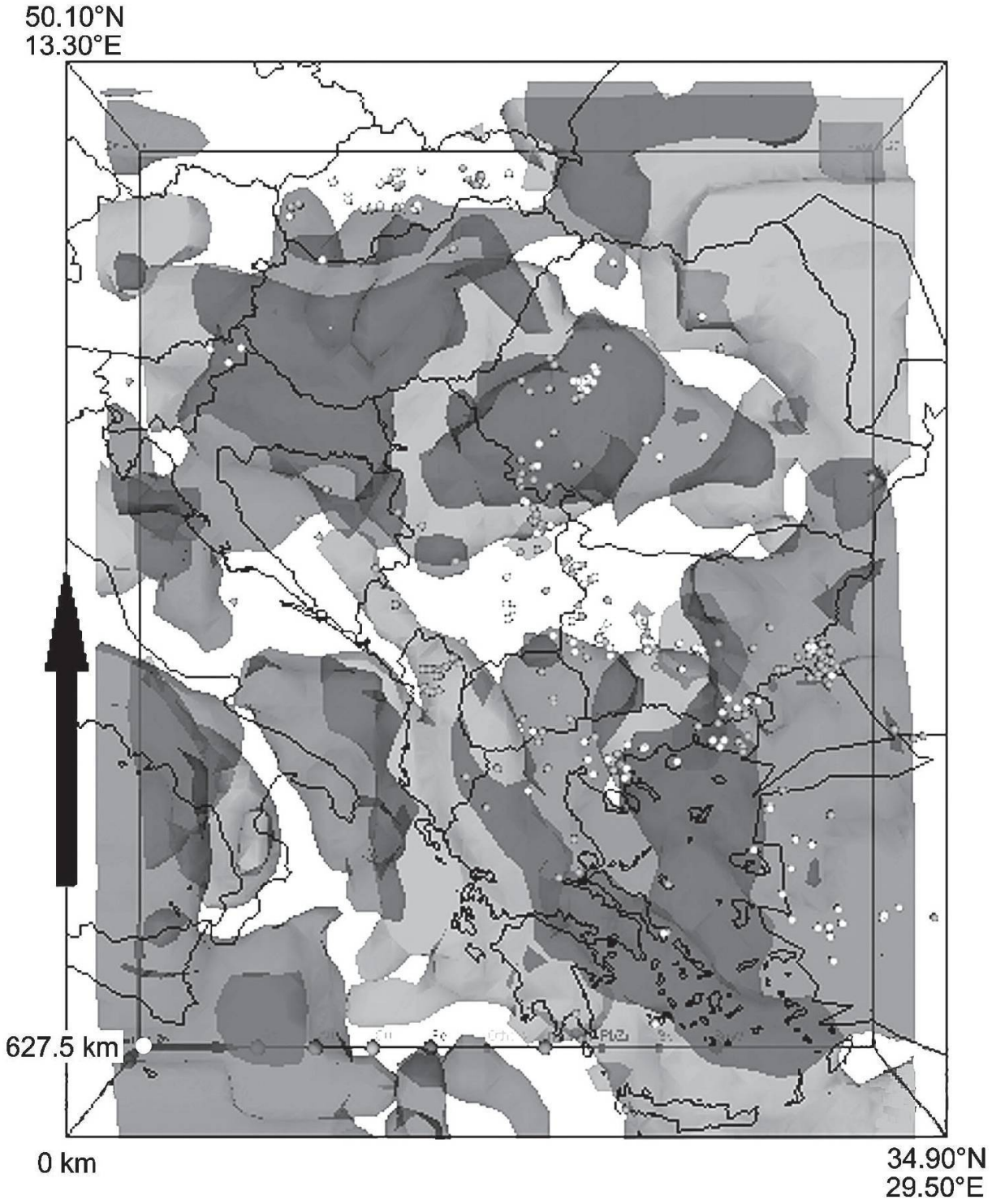

Fig. 5 3D visualization of seismic tomography below southeastern Europe viewed from above. Light gray indicates the 1% anomaly body, gray indicates the –1.5% anomaly body, darkest gray highlights the zones where the –1.5% bodies overly the 1% bodies. Dots show distribution of gold and copper deposits.

volume, and geometries of the observed phenomena, such as the high velocity anomalies marking the East European Platform, the continuation of the Hellenic subduction zone from a shallow dipping zone, to a moderately dipping zone, to a nearly horizontal segment below 600 km (towards the 660 km discontinuity); and a similar dense portion below 600 km underlies the Pannonian basin (Fig. 4). Low velocity anomalies are dominantly present at very shallow levels below the Aegean Sea (including western Anatolia) and significantly, but less extensively as for the Aegean region, at shallow levels below the Pannonian basin. As such, the 3-D visualization provides a quantitative follow-up to the studies of de Boorder et al. (1998) who investigated the correlation between late orogenic mineralization and shallow low velocity anomalies deduced from mantle tomogra-

phy. Figure 5 shows the distribution of copper and gold deposits (dots) over the high velocity (light gray, indicating the 1% isobody) and low velocity (gray, indicating the –1.5% isobody) anomalies. The image shows that known Neogene gold and copper districts are above or very near to the shallow positioned –1.5% low velocity isobodies. The image suggests that underlying (subducted) lithosphere obstructs the emplacement of deposits (e.g. Aegean arc and mainland Greece), unless this subducted lithosphere has been positioned at/around the 660 km discontinuity (Rhodope and Apuseni regions). Geodynamically this observation can be explained by the insufficient influx of asthenospheric heat in the narrow mantle wedges above shallow subducted lithosphere.

1.5. Mineral deposits

About 3090 mineral occurrences are presently incorporated in the database. This inventory is at a good level for almost all the countries, except for Austria and Poland which are under process of completion. Beside the general information for an occurrence (country, location, status, main commodity, references), available data are also stored about the stratigraphic age of the mineralization and its host rocks, the mineralogy of the mineralization and its gangue, as well as the type of associated alteration, the reference deposit type(s) and the morphology of the ore bodies, and the economic figures recorded per commodity and by ore type(s).

For the occurrences with known ages (a third of the total), it appears that most are of Cenozoic age (50%) or of Mesozoic age (40%), whilst the rest is of Paleozoic age and very rarely of older age (Fig. 6). The latter mainly concern Fe and/or Mn occurrences, like the ones hosted by the banded iron formation in former Yugoslavia and Romania, or some industrial rocks and minerals. The Neogene and the Cretaceous appear to be the two peak periods for mineralization. Obviously, this time distribution is a direct consequence of the relatively young geodynamic evolution of the Alpine-Balkan-Carpathian-Dinaride Belt (see also Heinrich and Neubauer, 2002; Földessy, 2002; Lips, 2002 and Neubauer, 2002).

When looking at the deposit types and the commodities concerned (Fig. 7), the following points can be underlined for several main commodities:

Gold and silver

A first important period of formation for Au–Ag deposits is during the Cretaceous (e.g. Chelopech in Bulgaria, Musariu in Romania, Bor district in Serbia). The dominant period of formation is during the Neogene and Quaternary. Quaternary deposits are of placer type, none of them being of economic importance. They are mostly reported

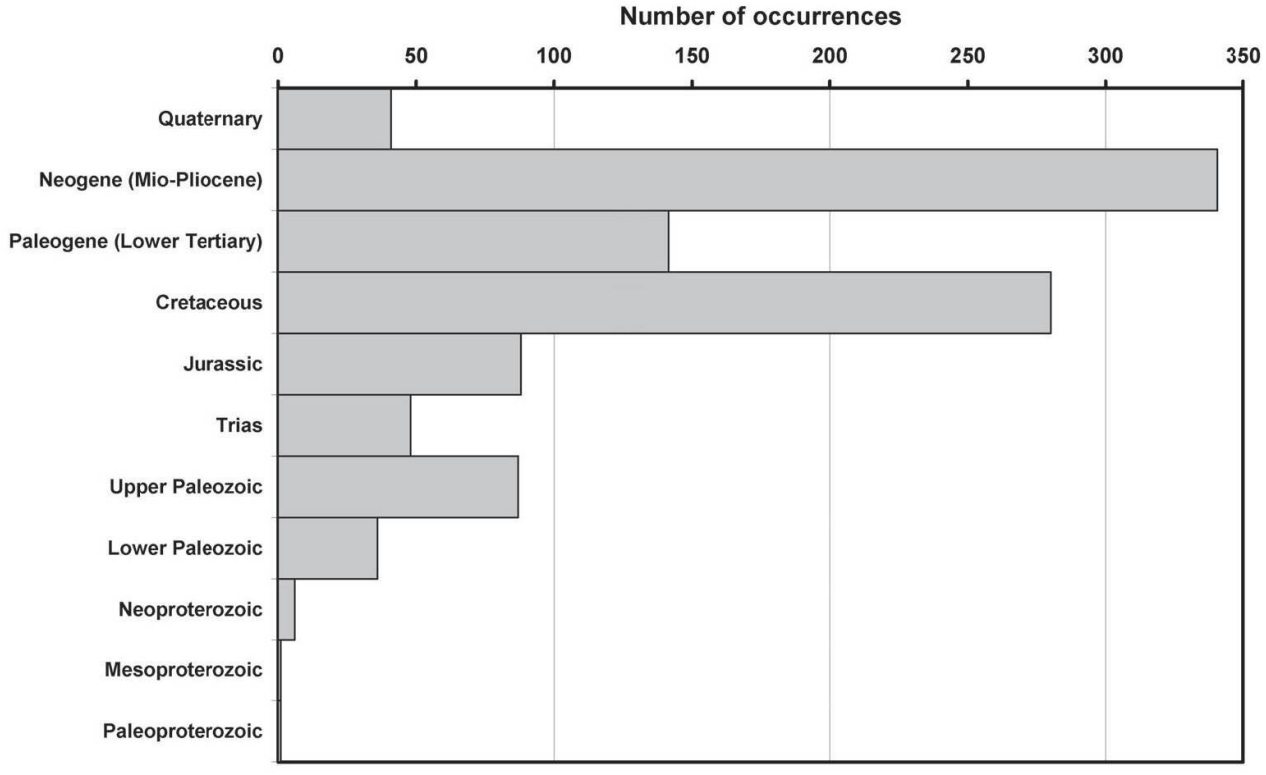

Fig. 6 Stratigraphic distribution of mineral occurrences (information available for 1070 of the 3090 mineral occurrences currently listed in the database).

in Bulgaria and NE Greece. Neogene occurrences belong either to the epithermal or porphyry-related type and are linked to the Tertiary volcanic and magmatic events. Some of these occurrences are of large economic size (Kisladag project in Turkey, Kremnica district in Slovakia, Rosia Montana in Romania, and Skouries project in Greece).

Lead and zinc

Here again, the maximum period of formation of the Pb–Zn occurrences corresponds to the Cretaceous–Tertiary ages, with an increasing activity from Cretaceous to Neogene. This mineralization is also magma-related, with some important hydrothermal and replacement type deposits (Madan, Laki, Madjarovo, and Davidkovo districts in Bulgaria; Kopaonik and Trepca districts in Serbia – with the Stari Trg, Belo Brdo, Novo Brdo, Ajvalija deposits; Asarcik in Turkey). The older and fewer occurrences are of very different type, like the Triassic sedex type of the Brskovo ore field (Brskovo, Zuta Prla deposits) in Serbia, and the Cambrian volcanogenic massive sulphide type of Baia Borsa deposit in Romania.

Copper

Cu occurrences are relatively abundant and their time distribution is slightly different from the previous ones, with a peak during Jurassic and Cretaceous, and a decreasing number of occurrences through the Tertiary. Jurassic and Cretaceous copper occurrences mostly belong to the volcanogenic massive sulphide (VMS) type, including the ophiolite-hosted VMS of Albania (Jurassic) and Cyprus (Late Cretaceous). Only few VMS occurences are known from other countries (e.g. Kure Asikoy, Murgul Maden or Madenkoy in Turkey). Through Late Cretaceous and Early Tertiary, the volcanic and magmatic events are also responsible for copper mineralization associated with Au–Ag–Pb–Zn. The typical deposits are of epithermal, porphyry or skarn-replacement type (e.g. from the Late Cretaceous porphyry and hydrothermal deposit of Bor in Serbia, the Moldova Nouà deposit in Romania, both with skarn and porphyry types, the porphyry deposit of Assarel in Bulgaria, to the Eocene epithermal and porphyry deposits of Recsk in Hungary).

Iron and manganese

Iron occurrences are widespread during the Mesozoic, much less during the Cenozoic, and are mostly linked to sedimentary or volcano-sedimentary rocks: the Rudabánya district in Hungary, related to sedimentary rocks (Ladinian), the oolitic iron mineralizations of Bulgaria (Neshkovtsi, Gradetz, Chiflika, Jurassic) and Serbia (Gamzigrad, Cenomanian), the combined Fe–Mn occurrences of Bosnia Herzegovina (Omarska, Pliocene; Ljubija, Carboniferous; Vares, Triassic), Bulgaria (Obrochishte, Oligocene) or Macedonia (Tajmiste, Devonian). The Late Cretaceous period was also favourable for the development of laterite-related iron mineralization, like those of Albania (Prrenjas), Turkey (Payas), or Serbia (Stimlje, Topola). Manganese mineralizations are well developed in several sedimentary basins like the Early Jurassic Úrkút basin in Hungary, or can be found associated to jasper levels in late Cretaceous formations (Bulgaria and Turkey). There are also several iron occurrences developed as magnetite skarns associated with the magmatic events of Late Cretaceous to Tertiary ages: Masca Bàisoara in Romania (Paleocene), Divrigi in Turkey (Paleogene), Kroumovo, Martinovo in Bulgaria (Late Cretaceous), Ayazmant, Catak in Turkey (Late Cretaceous).

Aluminium

The Cretaceous is an important period of formation of bauxite under tropical conditions. For example, almost all the bauxite deposits of Hungaria formed at this time in karst structures in carbonate rocks (Halimba, Csabpuszta, Iharkút, Fenyöfö). Hungaria is the main country for bauxites, but several occurrences can be found also in Bosnia Herzegovina (Bosanska Krupa, Mostar), Greece (Desfina Distomon, Parnasse Giona), or Serbia (Grebnik, Bijele Poljane).

Uranium

There are two very distinct periods of formation of uranium mineralization. During the Late Paleozoic, uranium enrichment probably stemmed from Variscan granitoids, and was mostly associated with mesothermal shear-zone systems (Carboniferous Bukhovo deposit, Bulgaria; Late Paleozoic Krásno-Horní Slavkov deposit, Czech Republic), or with felsic and alkaline plutonic rocks (Carboniferous Bukhovo deposit, Bulgaria). Cretaceous and Tertiary occurrences are mainly hosted by uraniferous sandstones (Eleshnitsa, Bulgaria; Stráz and Hamr, Czech Republic; Zirovski Vrh in Slovenia).

Coal and Lignite

Coal deposits formed during three main periods, lignite being present mainly during the most recent one: Late Carboniferous (Central Bohemian Basin, Late Silesian Basin, Melník Basin, Plzen and Radnice Basin in Czech Republic; Svoge in Bulgaria; Zonguldak in Turkey), Early Jurassic (Zobák in Hungaria), and Tertiary, with numerous deposits in all the countries.

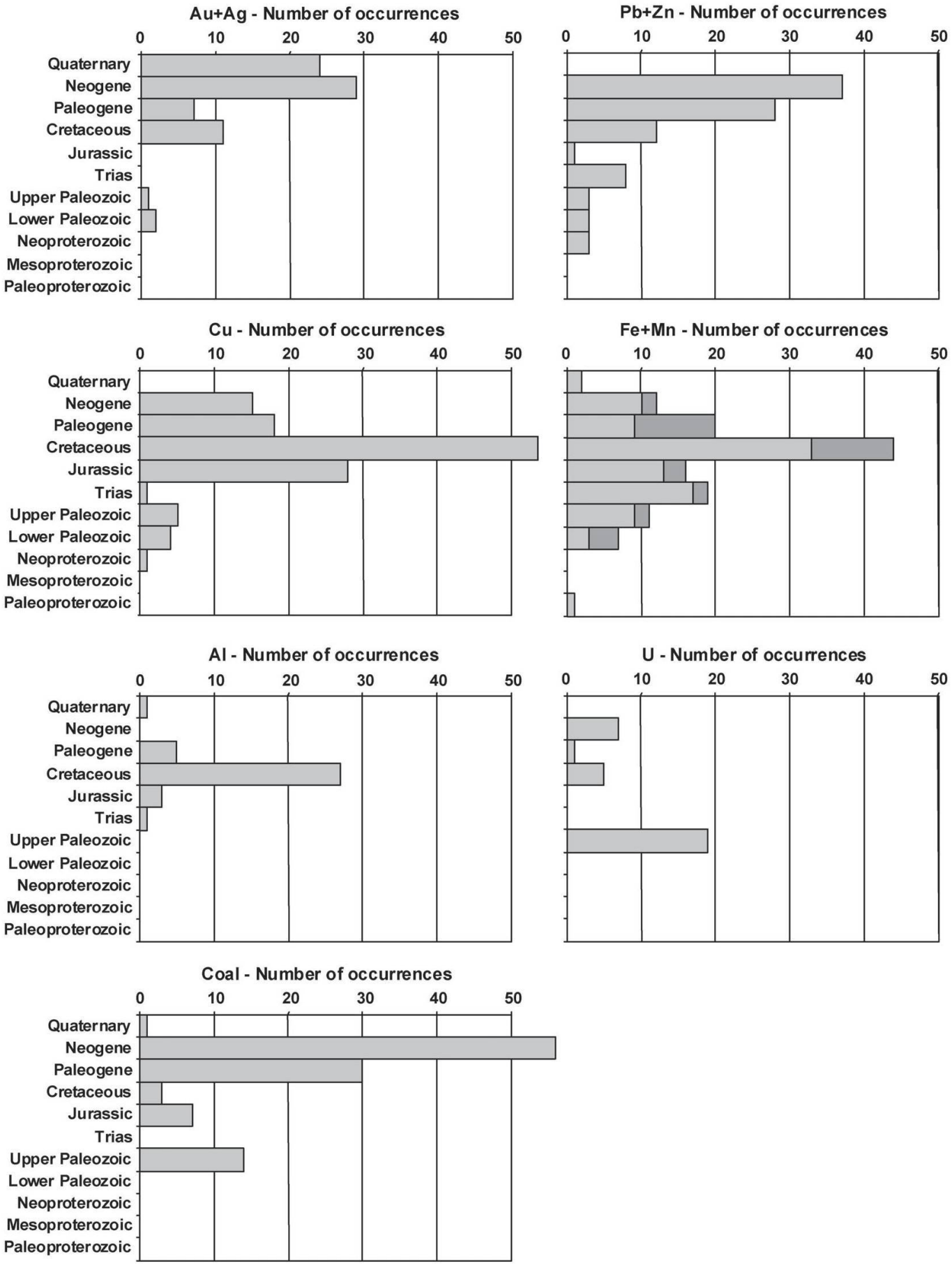

Fig. 7 Distribution of the occurrences through time for selected substances (Au+Ag: 73 occurrences; Pb+Zn: 95 occurrences; Cu: 200 occurrences, the maximum peak is at 128 occurrences; Fe+Mn: Fe 97 occurrences, in light gray, Mn 35 occurrences, in dark gray; Al: 37 occurrences; U: 32 occurrences; Coal: 174 occurrences, the maximum peak is at 119 occurrences).

Petroleum and gas resources

Vernet (2001) has shown that they are hosted by Neogene foredeeps and post-orogenic basins, like the Transsylvanian basin (Romania), the Pannonian basin (Croatia, Hungaria, Romania), and several molassic basins along the Carpathian arc (Slovenia, Poland and Romania); the source rocks rank from Triassic to Neogene.

The genesis of the greatest part of precious and base-metal mineralization is directly related to the geological evolution of the Tethys and the development of collision zones during the Alpine orogenic cycle (Mitchell, 1996; Lips, 2002). Volcanogenic massive sulphide occurrences, which are Cu dominated, were syngenetic to the formation of oceanic crust during the Jurassic and Late Cretaceous, corresponding to the rifting of Pangea and formation of new oceans. Ophiolite-hosted chromite occurrences also formed at the same time, deeper in the mafic-ultramafic complexes of the oceanic crust. Porphyry and epithermal type occurrences, bearing Au–Ag–Pb–Zn–Cu mineralizations, stemmed from the volcano-plutonic events taking place during the stages of closure of the Tethys, subduction and the passage to continental collision, from Late Cretaceous to Pliocene. Two successive major stages are generally distinguished, marked by the formation of magmatic belts (Mitchell, 1996). The time distribution of the magmatic related mineralizations clearly underlines these two events: the first one occurred during the Late Cretaceous to Earliest Paleogene, and the second during the Neogene.

2. Using GIS Central Europe

2.1. Application to mineral resources understanding and research

The completion of many of the basic information layers of the GIS – a rather unrewarding, time consuming and thus costly phase – allows one to start to fully use the system. The release of the homogeneous geological synthesis for the whole ABCD-GEODE region serves as an ideal basis for regional scale geodynamic investigations. The possibility to display over 3000 mineral deposits (carefully described in about 40 fields, filled by data entries from in-house hierarchical lexicons which integrate the latest developments and knowledge) over the geological layer allows to further investigate the spatial distribution of deposits, to realize sophisticated queries and to elaborate thematic documents. This contribution to metallogenic thinking is further enhanced by the integration of the mineral database with the geochronology layer which synthesizes all the published information after a careful evaluation of its quality. The satellite imagery layer with a 1 × 1 km resolution SPOT4 VEGETATION® image contributes to the identification of major crustal discontinuities likely to have controlled the circulation of hydrothermal fluids and therefore the location of mineral deposits. Essential geophysical data layers are provided through the compilation of the gravity data, allowing to derive different enhanced layers presenting calculated Bouguer anomalies, isostatic correction and corresponding residual anomalies, vertical gradients, and geophysical discontinuities, again contributing to better constrain the role of crustal structures in the distribution of hydrothermal systems – regionally with the topo-isostatic residual anomaly map and locally with the vertical gradient of the topo-isostatic residual anomaly map. In the same way, but at the continental and lithospheric scale, the 3-D tomography layer contributes to the understanding of the relationship between the geophysical and geodynamics processes and the localization of mineralizing phenomena.

The above inventory of ages of mineralization (Fig. 7) presents a relatively simple but informative way to highlight "metalliferous peaks" over geological time. Similarly, metal distribution maps can be produced to highlight the geographic areas that host most of a certain substance, irrespective of the age and the style of mineralization. Figures 8 to 10 present such metal distribution maps for gold and copper. After presentation of the deposits that have sufficient economic information (estimated production, reserves, resources) to arrive at an estimate of the metal potential of gold and/or copper (filled circles in Fig. 8), density calculations were carried out within a radius of 25 km around every indexed deposit (Figs. 9 and 10). Taking into consideration the heterogeneity of the distribution for indexed gold bearing deposits the resulting map for gold (Fig. 9) shows the dispersed gold rich regions along the northern Carpathians from west to east from Slovakia into northern Romania, in Albania, and in western Anatolia. Subsequently it highlights the 5 areas with gold densities approaching 1 t/km^2. These areas occur from north to south in the Apuseni, Bor, Panagyurishte, and Chalkidiki districts, and around Kisladag. A similar calculation for all copper bearing deposits (Fig. 10) returns a picture which is largely dominated by the similar heterogeneous distribution of indexed deposits presenting again the northern Carpathians and northern Albania with moderate copper distributions. The highest copper anomalies are produced by the

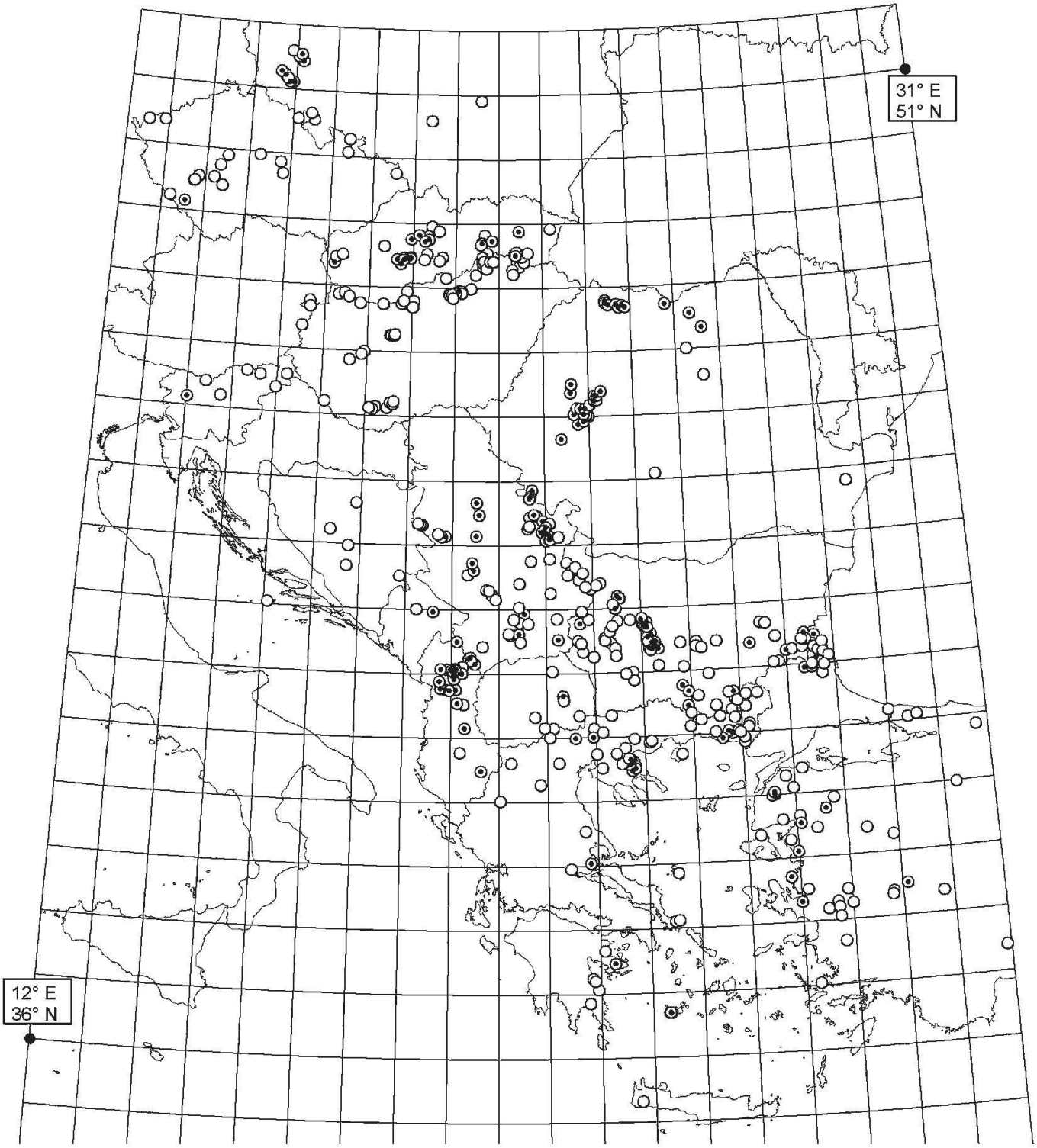

Fig. 8 Index map of all copper and gold bearing deposits (open circles) in the GIS (some countries await completion). Deposits with sufficient economic information (filled circles) have been used for gold and copper density calculations (Fig. 9 and 10).

porphyry copper deposits with copper densities above 1 kt/km^2. The only extremely high copper density is positioned in the Bor district with values between 10 and 20 kt/km^2, an anomaly which is comparable with the Polish Kupferschiefer (in the northwest of the image).

2.2. Application to mineral potential calculation and mapping

The development of the GIS base layers being completed, a more sophisticated equivalent to the above metal distribution calculations is currently undertaken. This "mineral potential mapping" subdivides areas according to metal or mineral fa-

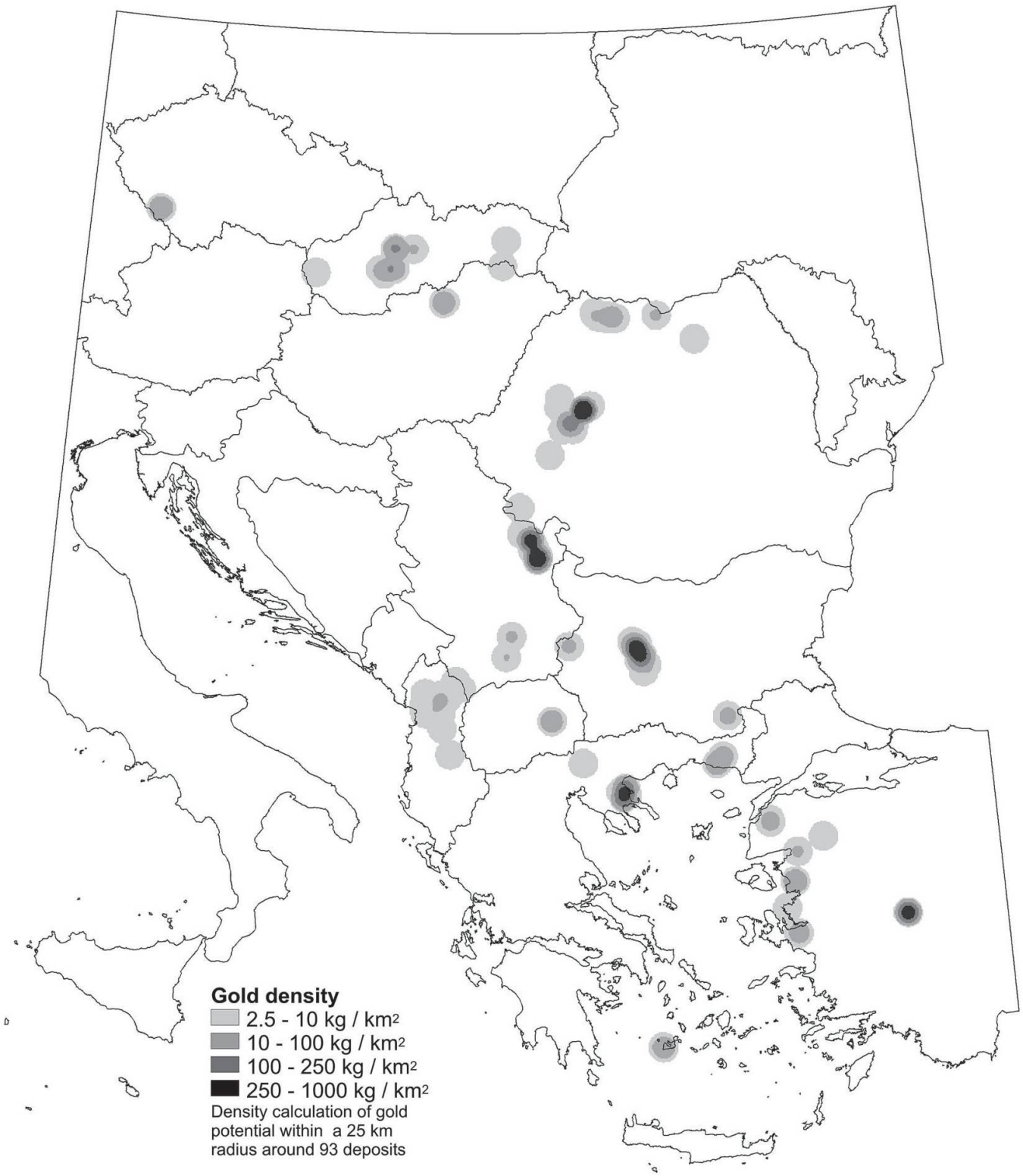

Fig. 9 Gold density map, indicating the distribution of gold (in kg per km^2) averaged over a radius of 25 km around 93 deposits with economic information.

vorability and may be carried out in commercial exploration programs or by governmental mineral resource assessments. The ability of a GIS to combine spatial data from different sources contributes significantly to identify spatial associations of the data, and to use models for analysis and prediction of the spatial phenomena (e.g. Bonham-Carter et al., 1989; Bonham-Carter, 1994; Burrough and McDonnell, 1998). The dedication of a GIS to mineral potential mapping is classically a three–step approach (e.g. Bonham-Carter, 1994; Knox-Robinson and Wyborn, 1997): (i) data identification and data organization, (ii) data quantification and data processing, and (iii) data integration and data modeling. The development of Data Mining and Artificial Neural Networking

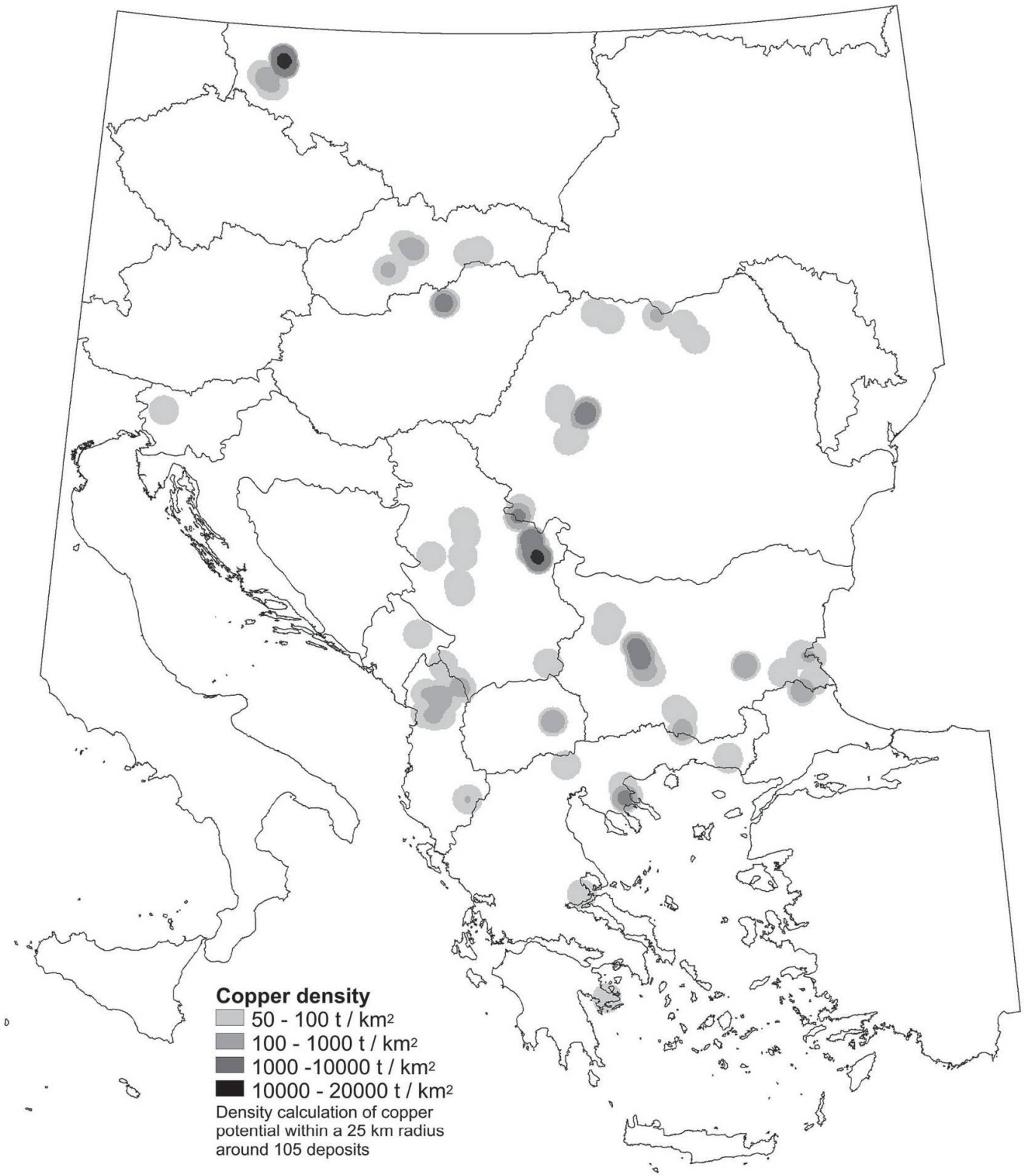

Fig. 10 Copper density map, indicating the distribution of copper (in t per km^2) averaged over a radius of 25 km around 105 deposits with economic information.

techniques and their application to spatial databases allow an alternative approach. They represent an adaptive computing system that can learn from the data to conduct specific tasks (e.g. by characterization or association). Unlike the above conventional three-step approach, the computing system can analyze all data simultaneously.

In the past decade, mineral potential mapping using a GIS has been applied by various research groups and involved different ore deposit models (Table 4). Models for predicting mineral potential, based on statistical relationships or on heuristic relationships, are examples of empirical models (in contrast to conceptual models; Knox-Robinson and Wyborn, 1997). The assignment of

Table 4 Summary of data-driven and knowledge driven studies for mineral potential mapping highlighting the different scale of this study in contrast to previous studies.

Reference	Study	Area	Surface	Scale	Deposits
Wright and Bonham-Carter, 1996	VHMS favourability mapping	Manitoba, Canada	150 km^2	1:50,000	16 deposits
Raines, 1999	Prediction of epithermal deposits	Great Basin, USA	less than 330 km^2		415 deposits as training sites
Knox-Robinson and Groves, 1997; Groves et al., 2000	Prediction of orogenic gold	Yilgarn block, Australia	less than 15,000 km^2		230 known Au deposits (including 150 for verification) selected from 2000 deposits
Carranza and Hale, 2000	Estimation of gold potential by weight of evidence modelling	north Philippines	400 km^2 (rasterized in 100m x 100m)		82 occurrences
		OUR ANDEAN STUDIES			
Billa et al., 2002; 2004	Estimation of gold potential by a knowledge driven approach (or expert guided "data-driven approach")	Central Andes	less than 2,000,000 km^2	Final synthesis of GIS Andes at 1:2,000,000	113 Neogene epithermal and porphyry Au deposits
Salleb and Vrain, 2000	Estimation of metal potential and derivation of new rules (in hierarchy) by Data Mining	Andes	less than 4,000,000 km^2	Final synthesis of GIS Andes at 1:2,000,000	441 Neogene deposits
Bougrain et al., 2002, 2003	Estimation of metal potential and derivation of new rules (in hierarchy) by Neural Networking	Andes	less than 4,000,000 km^2	Final synthesis of GIS Andes at 1:2,000,000	441 Neogene deposits and different non-deposit populations (corpi of 634, 653, 254, 238)
		OUR CURRENT EUROPEAN STUDIES			
	Estimation of metal potential by knowledge driven and data driven approaches	*SE Europe*	*less than 2,000,000 km^2*	*Final synthesis of the GIS at 1:1,500,000*	*100 to 200 deposits of a certain type, containing a certain substance and/or of a certain age*

weights to the different attribute information can either be carried out using statistical criteria, or the weights can be estimated on the basis of expert opinion. The approaches can be subdivided into "data-driven" and "knowledge-driven" models (Bonham-Carter 1994; Harris et al., 2001). In data-driven modeling, the various input maps are combined using models such as logistic regression, weights of evidence, or neural network analysis. Data-driven approaches require that prior knowledge exists in the form of known mineral deposits or occurrences for the study area. Knowledge-driven approaches rely on the geologist to weigh the importance of different data layers, and include the use of fuzzy logic, Bayesian probability and Dempster-Shafer belief theory (Bonham-Carter, 1994). Conceptual mineral deposit models, containing all typical characteristics of a certain type of deposit, may contribute in data selection and data modeling, in deciding which features to enhance and extract as evidence, and in deciding how to weigh the relative importance of evidence.

The principal advantage of weights of evidence modeling is that the method is well defined, reproducible, objective (avoids the subjective choice of weighting factors), and provides a quantitative measure of confidence (Raines, 1999).

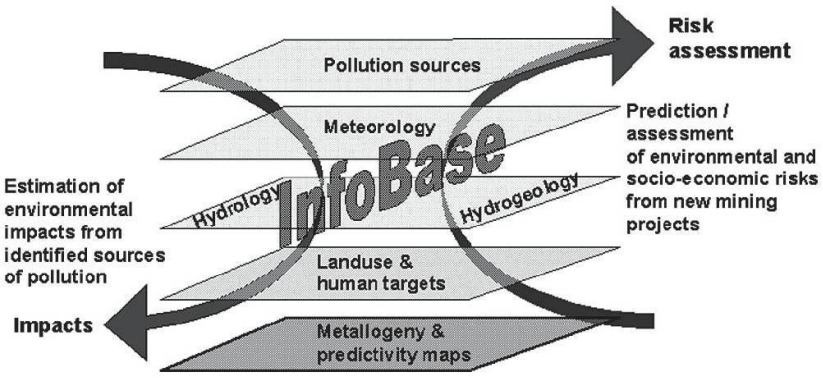

Fig. 11 Two areas of application for the "Environment" GIS module: (1) descriptive, (2) predictive.

Fuzzy sets (Zadeh, 1965) have been introduced to deal with inexact concepts in a definable way (e.g. Burrough and McDonnell, 1998). The fuzzy set theory has been applied to mineral exploration, e.g. by An et al. (1991) indicating that the method can adequately represent and manipulate imprecise and incomplete information. Data mining is defined as a process of extracting implicit unknown and potentially useful data from a GIS (Salleb and Vrain, 2000). Like other statistical approaches, a neural network requires the construction of a training set that is representative of both deposits and so-called "non-deposits", to allow discrimination between the two modalities (Bougrain et al., 2002, 2003).

Most studies dealing with the prediction of mineral potential have focussed on the distribution of deposits on a regional or district scale. In contrast to these studies, our studies – as for the Andes – focus on the distribution of deposits on a continental scale (Table 4). Problems arising from this approach are the loss of detailed phenomena by homogenization of the thematic layers, scale differences in resolution of the GIS and the scale at which individual deposits are controlled. In turn, by combining the scale at which the crust responds to geodynamic evolution and the observation scale of individual ore deposits, the continent-scale view aspires to identify and further quantify the continental-scale controls beyond the controls of individual deposits (e.g. crustal-scale faults and shears may provide a strong control on the location and the size of the deposit; or, convergent margin evolutions may influence the distribution of deposits). This quantitative assessment of a continent-scale GIS aims to characterize the optimal resolution for continent-scale metallogenic syntheses.

2.3. Application to environmental assessments

The georeferenced integration with metallogenic syntheses and prediction maps enables risk assessment and impact studies in relation to the mineral extractive industry (Fig. 11, Cassard and Itard, 2003). The objective of current research is to combine geological and metallogenic data with information on land-use, hydro(geo)logy, meteorological variations, and air- and water-quality monitoring (module 3, Table 1). The combination of information allows to regionally assess the impact of existing extracting industries and to predict the risks linked to new mining ventures. The basic assumption is that a good knowledge of such impact will lead to an environmentally safe development of this essential economic sector (Itard et al., 2002). The InfoBase structure provides a relation between minerals and their respective heavy-metal content, an estimation of mining waste and a theoretical heavy-metal signature for each deposit type, as well as a neutralization capacity for all host rock lithologies. Optimal integration of this information enables to compute a heavy-metal risk index for each deposit and to construct an Acid Mine Drainage risk map (Fig. 12). Using the DEM and the satellite imagery, regional risk maps for erosion, landslides and flooding can be created, and can be completed by a rainfall level map. Further data combination will ultimately lead to a ranking of regional risks, taking into account the pollutants, the possibilities of their transfer within the environment, and their toxicity.

3. Conclusions

Developing GIS Central Europe represents a vast synthesis effort which can now be enhanced through current research work such as a GIS-supported study to correlate geodynamic processes and ore deposit formation over time (Lips et al., 2002b). This research focusing on the evolution of the lithosphere at convergent continental margins identifies secondary thermal and mechanical processes that accompany the primary process of

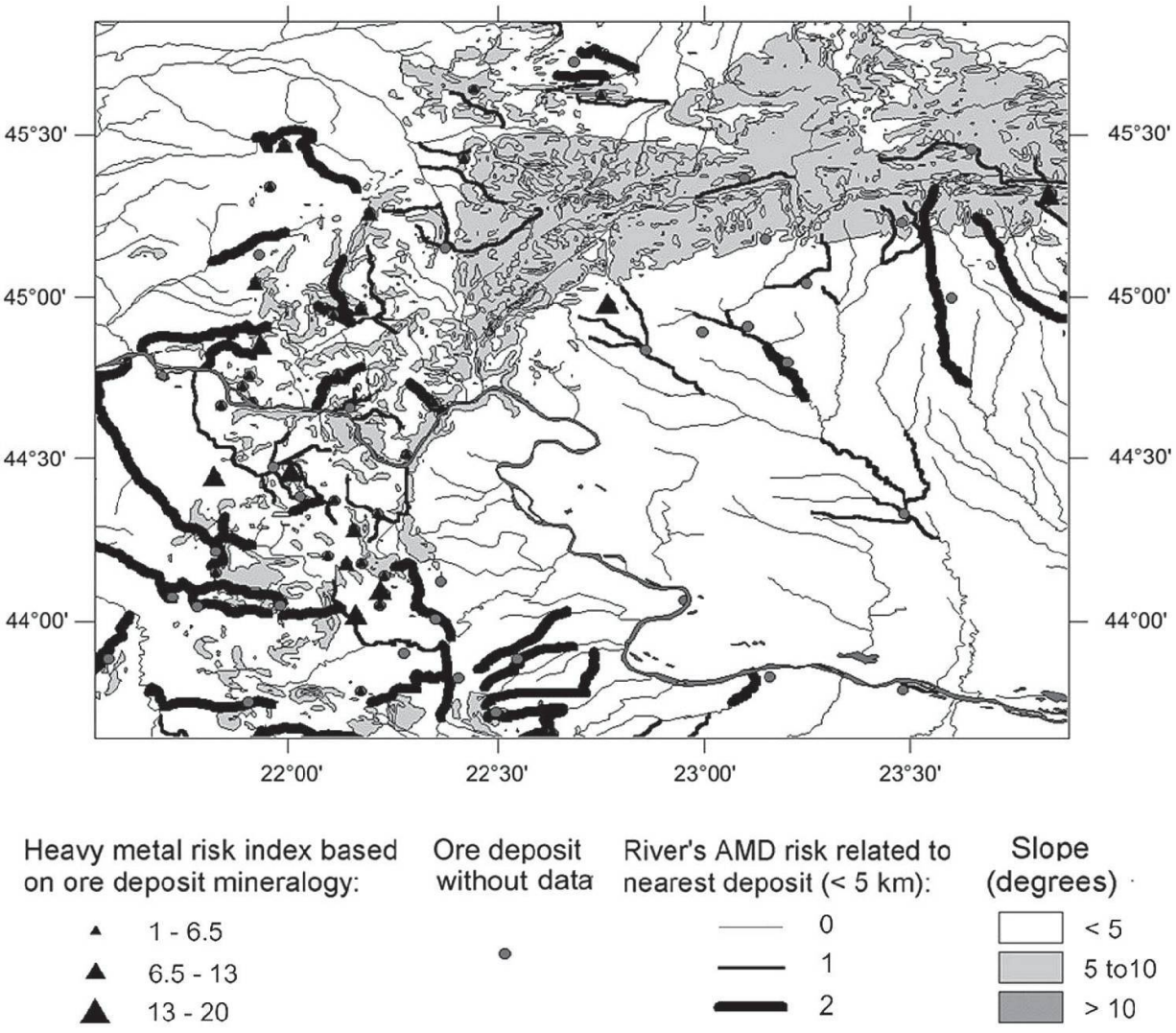

Fig. 12 Romania and Serbia: Presentation of a heavy-metal risk index for each deposit and of an Acid Mine Drainage (AMD) risk map.

subduction. Such secondary effects have been recognized as the possible trigger of the magmatism, regional crustal extension, and enhanced flow of heat and fluids in the crust. Lithospheric dynamics thus may have played a vital role in the formation and localization of ore deposits. The integration of all data associated with individual ore districts and with regional geodynamics in a single orogenic system is the primary feature of BRGM's continental-scale GIS study.

Establishment of the temporal and spatial constraints of the lithosphere-scale mechanisms, as well as detailed information on the timing of the mineralizing processes, are the first steps to understand the potential geodynamic causes of relatively short-lived regional igneous and hydrothermal ore-forming events. The GIS system can subsequently be used to quantitatively test the applicability of present genetic models on different scales (from ore district scale, to regional scale and vice versa). Modern data processing, using procedures such as data mining and neural network analysis, also allows the extraction of new relational rules (Lips et al., 2002a). Thus, new constraints can revise existing models or new models may replace the existing models. Step-by-step, the system allows the user to improve the present ore genesis models and to bridge the gap between the different scales at which ore genesis and geodynamics operate, evolving from a descriptive process to a predictive system.

The data analysis and synthesis, required to arrive at the different thematic layers, already highlight parameters that may be tentatively linked to ore deposit formation and localization. In the geophysical compilations the assessment and compilation of published heat flow data shows a large anomalous area of high heat flow, located within the Pannonian basin, adjacent to a region of anomalously low heat flow values (east Carpathians). Such high contrasts in the thermal regime in the crust may play a role in ore genesis. The compilation of multisource gravity information has returned enhanced gravity maps, Bou-

guer and isostatic anomalies, gravity gradients and gravity discontinuities. Linked in with the earthquake epicenter distribution, these layers contribute to a better understanding of the crustal structure, regionally with the topo-isostatic anomaly map and more locally with the vertical gradient anomaly map. The present-day structure of the crust, completed by the structure of the lithosphere, e.g. with the 3-D seismic tomography visualization, allows to verify the region's geodynamic evolution.

The 3-D vizualization and its correlation with the heat flow thematic layer reconfirms the preferred positioning of Neogene (Au) deposits above shallow low velocity bodies (de Boorder et al., 1998). The visualization also suggests that subducted lithosphere underlying these low velocity bodies obstructs the emplacement of the deposits (e.g. Aegean arc and mainland Greece), unless this subducted lithosphere has been positioned at/around the 660 km discontinuity (Rhodope and Apuseni regions). Geodynamically this observation can be explained by the insufficient influx of asthenospheric heat in the narrow mantle wedges above shallow subducted lithosphere.

In relation to the geodynamic setting certain ore deposit types mark the tectono-magmatic evolution of the Tethys and the Carpatho-Balkan arc. Oceanic type mineralizations (chromite, Cu massive sulphides) formed during the oceanic rifting from Jurassic to Late Cretaceous, and hydrothermal-porphyry types (base- and precious-metal mineralizations) formed during two major stages, during the Cretaceous to Paleogene, and subsequently during the Neogene.

Principally the information system allows the multidisciplinary exploitation of databases from different scientific domains, the optimal (distant) consultation (e.g. GIS Central Europe on-line at: http://sigeurope.brgm.fr), and the further integration, analysis and dissemination, of the multi-source data, derived from geological, engineering, environmental, medical, legal and other sources. In this way the system can provide policy-makers and citizens in Europe with the scientific elements and the required technologies to spatially and temporally manage the natural resources and their related information. Additionally, it assesses the environmental and the socio-economic impacts related to the exploitation and transformation of mineral resources across Europe in the past and at present. As such the system provides a key to sustainability of the pan-European non-energy extractive industry in its relation to major societal issues.

Acknowledgements

GIS Central Europe was developed within the context of a BRGM R&D project entitled "Global Environmental & Metallogenic Syntheses" (GEMS). We would like to thank our Colleagues of the ABCD-GEODE Programme under the leadership of Derek J. Blundell, Christoph A. Heinrich and Franz Neubauer who helped us to develop some of the GIS Central Europe layers presented here, with a special mention to Tudor Berza, Hugo de Boorder, Cristiana Ciobanu, Nigel J. Cook, Fritz Ebner, Radoslav Nakov, Jakob Pamic, Kamen Popov, Ioan Seghedi, and Rinus Wortel. From the BRGM side, we are particularly grateful to Gabriel Courrioux and Jacques Vairon who were in charge of developing the GIS Central Europe 3-D models and to Claude Heinry and Francis Ralay for their invaluable help in preparing maps and illustrations. Detailed reviews by Hugo de Boorder and Thomas Driesner are acknowledged and have substantially contributed to improve the manuscript. This work is registered as BRGM contribution N° 2784.

References

An, P., Moon, W.M. and Rencz, A. (1991): Application of fuzzy set theory to integrated mineral exploration. *Can. J. Exploration Geophysics*, **27**, 1–11.

Bijwaard, H., Spakman, W. and Engdahl, E.R. (1998): Closing the gap between regional and global travel time tomography. *J. Geoph. Res.*, **103**, 30055–30078.

Bijwaard, H. and Spakman, W. (2000): Nonlinear global P-Wave tomography by iterated linearized inversion. *Geoph. J. Int.*, **141**, 71–82.

Billa, M., Cassard, D., Guillou-Frottier, L., Lips, A.L.W. and Tourlière, B. (2002): Assessment of GIS Andes: predictive mapping of Neogene gold-bearing magmatic-hydrothermal systems in the Central Andes. 5th Intern. Symposium on Andean Geodynamics, September 16–18, 2002, Toulouse, France; Extended Abstracts. Institut de Recherche pour le Développement Publisher, Paris 2002, 89–92.

Billa, M., Cassard, D., Lips, A.L.W., Bouchot, V., Tourlière, B., Stein, G. and Guillou-Frottier, L. (2004): Predicting gold-rich epithermal and porphyry systems in the central Andes with a continental-scale metallogenic GIS. *Ore Geology Reviews*, **25**, 39–67.

Bonham-Carter, G.F., Agterberg, F.P. and Wright, D.F. (1989): Weights of evidence modelling: a new approach to mapping mineral potential. In: Agterberg, F.P. and Bonham-Carter, G.F. (eds.): Statistical Applications in Earth Sciences, *Geological Survey of Canada*, **89-9**, 171–183.

Bonham-Carter, G.F. (1994): Geographic information systems for geoscientists – Modelling with GIS. *Pergamon Computer Methods in the Geosciences*, **13**, 398 pp.

Boorder, H. de, Spakman, W., White, S.H. and Wortel M.J.R. (1998): Late Cenozoic mineralisation, orogenic collapse and slab detachment in the European Alpine Belt. *Earth Planet. Sci. Lett.*, **164**, 569–575.

Bougrain, L., Bouchot, V., Cassard, D., Lips, A.L.W., Gonzalez, M., Stein, G. and Alexandre, F. (2003): Knowledge recovery for continent-scale metal exploration by neural networks. *Natural Resources Research*, **12**, 173–181.

Bougrain, L., Gonzalez, M., Bouchot, V., Stein, G., Cassard, D. and Alexandre, F. (2002): Knowledge recovery for continental-scale metal exploration by neural networks. Symposium on the Application of Neural Networks to the Earth Sciences: Seventh Int.

Symp. on Mineral Exploration (ISME-02), August 20–21, 2002, NASA Mofett Field, Mountain View, California.

Burrough, P.A. and McDonnell, R.A. (1998): Principles of geographic information systems. Oxford University Press, 333 pp.

Carranza, E.J.M. and Hale, M. (2000): Geologically constrained probabilistic mapping of gold potential, Baguio District, Philippines. *Natural Resources Research*, **9**, 237–253.

Cassard, D. (1999): GIS Andes: A metallogenic GIS of the Andes Cordillera. 4th International Symposium on Andean Geodynamics, October 4–6, 1999, Göttingen, Germany; Extended Abstracts. Institut de Recherche pour le Développement Publisher, Paris 1999, 147–150.

Cassard, D., Felenc, J., Hocquard, C., Joubert, M., Monthel, J. and Prévôt, J.C. (2001a): GIS Andes: Mining districts. EUG XI, April 8–12, 2001, Strasbourg, France, J. Conf. Abs., Vol. 6, (N° 1), p. 265.

Cassard, D. and Itard, Y. (2003): Metallogenic and environmental information systems: A modern tool for the sustainable development of mineral resources. In: Tvalchrelidze, A.G. and Morizot, G. (eds.): Mineral resource base of the Southern Caucasus and systems for its management in the XXI century, NATO Science Series, IV. *Earth and Environmental Sciences*, **17**, 167–180.

Cassard, D., Stein, G., Milesi, J.P. and Lips, A.L.W. (2001b): GIS Central Europe: the Metallogenic GIS of Central and South-Eastern Europe. In: Geodynamics and Ore Deposit Evolution of the Alpine-Balkan-Carpathian-Dinaride Province, ABCD-GEODE 2001 Workshop, Vata Bai, Romania, June 8–12, 2001, Abstract Volume, *Romanian Journal of Mineral Deposits*, **79**, (N° 2), 43–44.

Cermak, V., Kresl, M., Kucerova, L., Safanda, J., Frasheri, A., Kapedani, N., Lico, R. and Cano, D. (1996): Heat flow in Albania. *Geothermics*, **25**, 91–102.

Chalot-Prat, F. and Girbacea, R. (2000): Partial delamination of continental mantle lithosphere, uplift-related crust-mantle decoupling, volcanism and basin formation: a new model for the Pliocene-Quaternary evolution of the southern East-Carpathians, Romania. *Tectonophysics*, **327**, 83–107.

Courrioux, G., Nullans, S., Guillen, A., Boissonat, J.D., Repusseau P., Renaud X. and Thibaut, M. (2001): Volumetric modelling of Cadomian terranes (Northern Britanny, France): an automatic method using Voronoi diagrams. *Tectonophysics*, **331**, 181–196.

Földessy, J. (2002): Carpatho-Balkan belt: base- and precious-metal mineralization in volcanic rocks – a review. *Chronique de la Recherche Minière*, n° hors série, 47–53.

Groves, D.I., Goldfarb, R.J., Knox-Robinson, C.M., Ojala, J., Gardoll, S., Yun, G.Y. and Holyland, P. (2000): Late kinematic timing of orogenic gold deposits and significance for computer-based exploration techniques with emphasis on the Yilgarn Block, Western Australia. *Ore Geology Reviews*, **17**, 1–38.

Harris, J.R., Wilkinson, L., Heather, K., Fumerton, S., Bernier, M.A., Ayer, J. and Dahn, R. (2001): Application of GIS processing techniques for producing mineral prospectivity maps – a case study: mesothermal Au in the Wayze Greenstone Belt, Ontario, Canada. *Natural Resources Research*, **10**, 91–124.

Heinrich, C.A. and Neubauer, F. (2002): Cu–Au–Pb–Zn–Ag metallogeny of the Alpine–Balkan–Carpathian–Dinaride geodynamic province. In: Heinrich, C.A. and Neubauer, F. (eds.): Metallogeny of the Alpine–Balkan–Carpathian–Dinaride geodynamic province. *Mineralium Deposita*, **37**, 533–540.

Itard, Y., Geiller, M., Cassard, D. and Lips, A.L.W. (2002): Environmental dimension of a regional metallogenic synthesis: a way towards a sustainable extractive industry. GIS in Geology Int. Conference, Vernadsky SGM RAS, November 13–15, 2002, Moscow, Extended abstracts volume, 51–53.

Knox-Robinson, C.M. and Wyborn, L.A.I. (1997): Towards a holistic exploration strategy: using geographic information systems as a tool to enhance exploration. *Australian Journal of Earth Sciences*, **44**, 453–463.

Knox-Robinson, C.M. and Groves, D.I. (1997): Gold prospectivity mapping using a geographic information system (GIS) with examples from the Yilgarn block of western Australia. *Chronique de la Recherche Minière*, BRGM Publisher, **529**, 127–138.

Krus, S. and Sutora, A. (1986): Geophysical-geological Atlas of the Alpine-Carpathian mountain system. Rep. Archive, Geofyzika Brno.

Krolikowski, C. and Petecki, Z. (1995): Gravimetric atlas of Poland. Panstwowy Instytut Geologiczny.

Lips, A.L.W. (2002): Cross-correlating geodynamic processes and magmatic-hydrothermal ore deposit formation over time; a review on southeast Europe. In: Blundell, D.J., Neubauer, F. and von Quadt, A. (eds.): The timing and location of major ore deposits in an evolving orogen. *Geological Society, London, Special Publications*, **204**, 69–79.

Lips, A.L.W., Cassard, D., Bouchot, V., Billa, M., Salleb, A., Gonzalez, M., Bougrain, L., Vrain, C., Tourlière, B., Stein, G. and Alexandre, F. (2002a): Quantatitative assessments of a continent-scale metallogenic GIS by data-driven and knowledge-driven approaches to construct decision-aid documents. GIS in Geology Int. Conference, Vernadsky SGM RAS, November 13–15, 2002, Moscow, Extended abstracts volume, 74–76.

Lips, A.L.W., Cassard, D., Stein, G. and Milesi, J.P. (2002b): A GIS-supported study to correlate geodynamic processes and ore deposit formation over time. In: Marsh, E.E., Goldfarb, R.J. and Day, W.C. (eds.): Global Exploration 2002: Integrated Methods for Discovery, SEG Meeting, April 14–16, 2002, Denver, Colorado. Abstracts of Oral and Poster Presentations, p. 118.

Lemoine, F.G., Kenyon, S.C., Factor, J.K., Trimmer, R.G., Pavlis, N.K., Chinn, D.S., Cox, C.M., Klosko, S.M., Luthcke, S.B., Torrence, M.H., Wang, Y.M., Williamson, R.G., Pavlis, E.C., Rapp, R.H. and Olson, T.R. (1998): The Development of the Joint NASA GSFC and NIMA Geopotential Model EGM96, NASA TP-1998-206861, July 1998, 575 pp.

Mitchell, A.H.G. (1996): Distribution and genesis of some epizonal Zn–Pb and Au provinces in the Carpathian-Balkan region. *Trans. Instn. Min. Metall., sect. B, Applied Earth Sciences*, **105**, B127-B138.

Nemcock, M., Pospisil, L., Lexa, J. and Donelick, R.A. (1998): Tertiary subduction and slab break-off model of the Carpathian-Pannonian region. *Tectonophysics*, **295**, 307–340.

Neubauer, F. (2002): Contrasting Late Cretaceous with Neogene ore provinces in the Alpine–Balkan–Carpathian–Dinaride collision belt. In: Blundell, D.J., Neubauer, F. and von Quadt, A. (eds.): The timing and location of major ore deposits in an evolving orogen. *Geological Society, London, Special Publications*, **204**, 81–102.

Pfister, M., Rybach, L. and Simsek, S. (1998): Geothermal reconnaissance of the Marmara Sea region (NW Turkey): surface heat flow density in an area of active continental extension. *Tectonophysics*, **291**, 77–89.

Pollack, H.N., Hurter, S.J. and Johnson, J.R. (1993): Heat flow from the Earth's interior: analysis of the global data set. *Rev. Geophys.*, **31**, 267–280.

Raines, G.L. (1999): Evaluation of weights of evidence to predict epithermal-gold deposits in the Great Basin of the Western United States. *Natural Resources Research*, **8**, 257–276.

Salleb, A. and Vrain, C. (2000): An application of association rules discovery to geographic information systems. In: 4th European Conference on Principles of Data Mining and Knowledge Discovery in Databases (PKDD'2000), September 13–16, 2000, Lyon, France, 613–618.

Sandwell, D.T. and Smith, W.H.F. (1997): Marine gravity anomaly from Geosat and ERS-1 satellite altimetry. *J. Geophys. Res.*, **102**, 10039–10054.

Spakman, W. (1993): Iterative strategies for non-linear travel time tomography using global earthquake data. In: Iyer, H.M. and Hirahara, K. (eds.): Seismic tomography; theory and practice. Chapman and Hall, London, 313–339.

Tari, G., Dövényi, P., Dunkl, I., Horvath, F., Lenkey, L., Stefanescu, M., Szafian, P. and Toth, T. (1999): Lithospheric structure of the Pannonian basin derived from seismic, gravity and geothermal data. In: Durand, B., Jolivet, L., Horvath, F., and Séranne, M. (eds.): The Mediterranean Basins: Tertiary extension within the Alpine orogen. *Geological Society, London, Special Publications*, **156**, 215–250.

Vernet, H. (2001): Peri-Téthys et hydrocarbures. *Géochronique*, **79**, p. 52.

Wortel, M.J.R. and Spakman, W. (2000): Subduction and slab detachment in the Mediterranean-Carpathian region. *Science*, **290**, 1910–1917.

Wright, D.F. and Bonham-Carter, G.F. (1996): VHMS favourability mapping with GIS-based integration models, Chisel Lake-Anderson area. In: Bonham-Carter, G.F., Galley, A.G. and Hall, G.E.M. (eds.), EXTECH I, *Geol. Surv. Can. Bull.*, **426**, 339–376.

Zadeh, L.A. (1965): Fuzzy sets. *Information and control*, **8**, 338–353.

Zatopek, A. (1979): On geodynamical aspects of geophysical syntheses in Central Europe. In: Geodynamic investigations in Czechoslovakia, Final Report. Veda-SAV Bratislava, 91–104.

Received 3 July 2003
Accepted in revised form 2 April 2004
Editorial handling: A. von Quadt